

KSRP is critical in governing hepatic lipid metabolism through controlling *Per2* expression

Chu-Fang Chou,^{1,*} Xiaolin Zhu,^{1,†} Yi-Yu Lin,^{*} Karen L. Gamble,[§] W. Timothy Garvey,[†] and Ching-Yi Chen^{2,*}

Department of Biochemistry and Molecular Genetics,^{*} Department of Nutrition Sciences,[†] and Department of Psychiatry and Behavioral Neurobiology,[§] University of Alabama at Birmingham, Birmingham, AL 35294

Abstract Hepatic lipid metabolism is controlled by integrated metabolic pathways. Excess accumulation of hepatic TG is a hallmark of nonalcoholic fatty liver disease, which is associated with obesity and insulin resistance. Here, we show that KH-type splicing regulatory protein (KSRP) ablation reduces hepatic TG levels and diet-induced hepatosteatosis. Expression of period 2 (*Per2*) is increased during the dark period, and circadian oscillations of several core clock genes are altered with a delayed phase in *Ksrp*^{-/-} livers. Diurnal expression of some lipid metabolism genes is also disturbed with reduced expression of genes involved in de novo lipogenesis. Using primary hepatocytes, we demonstrate that KSRP promotes decay of *Per2* mRNA through an RNA-protein interaction and show that increased *Per2* expression is responsible for the phase delay in cycling of several clock genes in the absence of KSRP. Similar to *Ksrp*^{-/-} livers, both expression of lipogenic genes and intracellular TG levels are also reduced in *Ksrp*^{-/-} hepatocytes due to increased *Per2* expression. Using heterologous mRNA reporters, we show that the AU-rich element-containing 3' untranslated region of *Per2* is responsible for KSRP-dependent mRNA decay. These findings implicate that KSRP is an important regulator of circadian expression of lipid metabolism genes in the liver likely through controlling *Per2* mRNA stability.—Chou, C-F., X. Zhu, Y.Y. Lin, K. L. Gamble, W. T. Garvey, and C-Y. Chen. KSRP is critical in governing hepatic lipid metabolism through controlling *Per2* expression. *J. Lipid Res.* 2015. 56: 227–240.

Supplementary key words circadian rhythms • fatty acid synthesis • KH-type splicing regulatory protein • liver • nuclear receptors/sterol-regulatory element binding protein 1 • period 2 • ribonucleic acid turnover • steatosis • triglyceride

The liver plays a central role in lipid metabolism. In the postprandial state, the liver converts substrate into TG for local storage as well as export to peripheral tissues in the form of VLDL. This process is controlled by multiple metabolic pathways, and dysregulation of these pathways may lead to hepatic steatosis, which is characterized by excess

accumulation of TG in hepatocytes and is the hallmark of nonalcoholic fatty liver disease (NAFLD). NAFLD, the most common form of chronic liver disease, is strongly associated with obesity, type 2 diabetes, and insulin resistance (1, 2). Steatosis occurs when there is an imbalance between lipid availability, which includes fatty acid uptake coming from the hydrolysis of TG stored in adipose tissue and dietary fatty acids and de novo fatty acid synthesis, and lipid disposal via fatty acid oxidation and VLDL secretion (3–5). Studies in humans and rodents have revealed that excess accumulation of hepatic TG is mainly linked to increased delivery of NEFA from peripheral expanded adipose tissue to the liver and enhanced de novo lipid synthesis via lipogenic pathway in the liver itself while lipid disposal via β -oxidation and VLDL export have only minor contributions (6). Thus, elucidating the molecular mechanisms controlling hepatic lipid metabolism should lead to a better understanding of the biological basis of hepatic steatosis and aid its prevention.

Most living organisms display circadian rhythms in behavior and physiological processes such as sleep, feeding, metabolism, and body temperature. These rhythms are guided

Abbreviations: Aacs, acetoacetyl-coenzyme A synthetase; Acaca, acetyl-coenzyme A carboxylase alpha; Acadm, acyl-coenzyme A dehydrogenase, medium chain; Agpat2, 1-acylglycerol-3-phosphate *O*-acyltransferase 2; Agpat6, 1-acylglycerol-3-phosphate *O*-acyltransferase 6; ARE, AU-rich element; Arnt, aryl hydrocarbon receptor nuclear translocator; Bmal1, brain and muscle Arnt-like protein-1; Cpt1a, carnitine palmitoyltransferase 1a; Cry, cryptochrome; Dbp, D site albumin promoter binding protein; DD, constant darkness; Dex, dexamethasone; Dgat2, diacylglycerol *O*-acyltransferase 2; Elovl6, ELOVL family member 6, elongation of long chain fatty acids; eWAT, epididymal white adipose tissue; Gpat1, glycerol-3-phosphate acyltransferase, mitochondrial; HFD, high-fat diet; Hmgcr, 3-hydroxy-3-methylglutaryl-coenzyme A reductase; KSRP, KH-type splicing regulatory protein; LD, light/dark; Ldlr, low density lipoprotein receptor; MEF, mouse embryonic fibroblast; NCD, normal chow diet; Per, period; qPCR, quantitative PCR; Scd1, stearoyl-coenzyme A desaturase 1; SCN, suprachiasmatic nuclei; Slc27a2, solute carrier family 27 (fatty acid transporter) member 2; Slc27a5, solute carrier family 27 (fatty acid transporter) member 5; Srebp1c, sterol-regulatory element binding protein 1c; 3' UTR, 3' untranslated region; ZT, Zeitgeber time.

¹C-F. Chou and X. Zhu contributed equally to this work.

²To whom correspondence should be addressed.
e-mail: cchen@uab.edu

This work was supported by National Institutes of Health Grant GM068758.

Manuscript received 6 May 2014 and in revised form 12 December 2014.

Published, JLR Papers in Press, December 16, 2014

DOI 10.1194/jlr.M050724

Copyright © 2015 by the American Society for Biochemistry and Molecular Biology, Inc.

This article is available online at <http://www.jlr.org>

by external light-dark signals that are integrated through intrinsic central and peripheral molecular clocks (7, 8). In mammals, the central clock located in the suprachiasmatic nuclei (SCN) of the anterior hypothalamus and the peripheral clocks present in most peripheral tissues are controlled by a common transcriptional circuitry that results in cascades of gene expression with 24 h periodicity (9). The heterodimeric transcriptional factor complex of circadian locomotor output cycles kaput (CLOCK) and brain and muscle aryl hydrocarbon receptor nuclear translocator (Arnt)-like protein-1 (BMAL1) activates transcription of period (*Per*) and cryptochrome (*Cry*) genes (10–14). The resulting PER and CRY proteins interact with each other to form a repressive complex that translocates into the nucleus to inhibit CLOCK/BMAL1 transcription activity, resulting in the repression of the *Per* and *Cry* genes (7, 15–17). This core negative feedback loop is modulated by another interlocking feedback loop involving the orphan nuclear receptor, REV-ERB α , which is a direct target of CLOCK/BMAL1 and represses *Bmal1* transcription (18).

Accumulating evidence highlights intriguing interplays between circadian and metabolic pathways. Remarkably, animal studies and epidemiological evidence suggest that disturbance of circadian rhythms through environmental and genetic effects can lead to metabolic diseases, and mice with defective clock functions develop a number of pathological conditions including metabolic disorders (19–23). The interplay is exemplified by studies that examine gene expression profiles throughout the circadian cycle in metabolic tissues such as liver, skeletal muscle, and adipose tissue (24–27). In any given tissue, 3% to 10% of transcripts showed circadian rhythmicity. Many of them participate in common metabolic pathways such as metabolism of glucose, cholesterol, and lipid. These observations highlight the central role of circadian regulation in lipid homeostasis and suggest that disturbance of diurnal oscillations of lipid metabolism genes can result in an alteration in hepatic TG content. These are supported by the studies showing that *Clock* mutant and *Bmal1*-null mice develop hyperlipidemia and hepatic steatosis (19, 28) and that ablation of *Rev-erbs* and histone deacetylase 3 (*Hdac3*), both of which control the circadian expression of lipogenic genes, increases TG content in the liver (29, 30). In addition, *Per1/Per2*-null mice showed reduced liver TG levels (31), and hepatic TG concentrations were elevated in *Cry1/Cry2*-null mice (32).

KH-type splicing regulatory protein (KSRP) is a multifunctional RNA-binding protein involved in posttranscriptional regulation of gene expression including splicing (33), mRNA decay (34), primary microRNA (pri-miRNA) processing (35), and translation (36). In the control of mRNA decay, KSRP binds the AU-rich elements (AREs) in the 3' untranslated regions (3' UTRs) of inherently unstable mRNAs and promotes their decay by recruiting mRNA decay machineries (34, 37). KSRP has been demonstrated to be required for decay of reporter mRNAs containing various AREs from *c-fos*, *Tnfa*, and interleukin 8 (34, 38) and endogenous ARE-containing mRNAs in established cell lines (38–41). The in vivo function of KSRP in controlling mRNA decay and the associated phenotypes resulting from KSRP deficiency have

not been completely established. To do this, we have generated *Ksrp*-null mice and shown that type I IFN gene expression is upregulated in *Ksrp*^{-/-} cells and *Ksrp*^{-/-} mice in response to viral infection due to reduced mRNA decay (42). In the present study, we report that *Ksrp*^{-/-} mice exhibit increased expression of *Per2* and altered circadian clock in the liver. These mutant mice have reduced liver TG contents and are protected from diet-induced hepatic steatosis. Expression of genes involved in de novo lipogenesis is reduced in the livers of *Ksrp*^{-/-} mice. We further show that downregulation of *Per2* restores lipogenic gene expression and reverses the reduced TG levels in *Ksrp*^{-/-} hepatocytes, indicating that *Per2* is a negative regulator of lipogenesis. These findings suggest KSRP as a critical factor in governing hepatic lipid metabolism through regulation of circadian timing of lipogenic gene expression and as a potential therapeutic target to control hepatosteatosis.

MATERIALS AND METHODS

Animal studies

Generation of *Ksrp*-null mice in C57BL/6J background has been described (42). Mice were maintained under a 12 h light/12 h dark cycle and fed ad libitum a normal chow diet (NCD) or a high-fat diet (HFD) (Harlan Laboratories, TD.06415) containing 45% kcal from fat for 6–8 weeks. All experiments were performed using 10- to 16-week-old male mice. All animal studies were conducted in accordance with guidelines for animal use and care established by the University of Alabama at Birmingham Animal Resource Program and the Institutional Animal Care and Use Committee.

Behavioral and food intake analysis

Mice (10 weeks of age) were placed in individual running wheel cages, and activity was recorded using the ClockLab data collection system (Actimetrics, Wilmette, IL). Actograms were generated using 6 min bins of activity and double plotted for ease of examination. Behavior was analyzed across 10 days for light/dark (LD) analysis and 14 days of activity for constant darkness (DD) analysis after the mice had been in constant conditions for 12 days. The free-running period (τ) was determined by Chi-square (χ^2) periodogram analysis. Food intake was measured using the Comprehensive Lab Animal Monitoring System.

Tissue and serum collection

Tissues were collected at 4 h intervals across the LD cycle. Sera were collected either at Zeitgeber time (ZT) 4 from mice fed ad libitum (fed condition) or at ZT4 from mice fasted for 16 h (from ZT 12 to ZT4).

Liver and serum lipid measurement

Lipids were extracted from liver (~100 mg) as described (43). TG concentrations in liver and serum were measured using Pointe Scientific Triglycerides Liquid Reagents (Fisher Scientific).

mRNA analysis

Total RNA was extracted by TRIzol (Invitrogen). For quantitative real-time RT-PCR analysis, total RNA (1 μ g) was reverse transcribed using random hexamers. Amplification was performed by using Roche LC480 Light Cycler and SYBR Green system (Roche). mRNA levels were normalized to that of β -actin or cyclophilin B mRNAs. The sequences of the primers are listed in Table 1.

TABLE 1. Real-time PCR primers

Gene	Forward	Reverse
Aacs	CAGCCTGTGTGTACCCAGTA	CGGCCACCTCCACTTTCTTGC
β -actin	GTTCCGATGCCCTGAGGCTC	CAGACAGCACTGTGTTGGCA
Acaca	ATCCACAATGCCAACCCCTGAG	CCTGGACCAAGCTGCGGATCT
Acadm	AGACGAAGCCACGAAGTATGC	TCATCAGCTTCTCCACAGGGT
Agpat2	ACGCAACGACAATGGGGACCT	GGTGGCCCTCATGGACTGGTA
Agpat6	GAGTGAAGTCTGCCATTGCCCT	GGCTGCGGTCCTCATGGTTTC
Bmal1	CCTCCCCCTGATGCCTCTTCT	TGCCTCATCGTTACTGGGACT
Cd36	GGAGCTGTTATTGGTGCAGTC	TGCTGTTCTTTGCCACGTCAT
Clock	CAGCTTCCTCAGTTCAGCAGC	TACTGTGGCTGGACCTTGGAA
Cpt1a	ACTATGTGTCTGTGGCGGGG	TTTTGGAAATGGCGGCTGAGGC
Cry1	AGCAGCAGCGGAATGGAGGG	CTGGGCATCCTCTTGCTGACT
Cry2	TTGGCATCTGTCCCTTCTCTGT	GCCCCGTTGGTCAGTTCTTCA
Cyclophilin B	AAGGTGCTCTTCGCGCGCCG	TGATGACACGATGGAACCTGGCTGT
Dbp	TGCTAATGACCTTTGAACCTGATCC	TGCATCTCTCGACTCTTGCTGCT
Dgat2	CAGCATCCTCTCAGCCCTCC	CAGCCAGGTGAAGTAGAGCA
Elovl6	CTCAGCAAAGCACCCGAACATA	TGACACAGCCCATCAGCATCT
Fasn	AGAGCCTGGAAGATCGGGTGG	GCACAGACACCTTCCCCTCAC
Gpat1	CTCTGCTGCCATCTTTGTGCCA	AGACACTCGCTTTTGCTGGT
Hmgcr	CAACGCCCACGCAGCAAACAT	CTCACCAGCCATCACAGTGCC
Ldlr	GGCAGAGGGAATGAGGAGCAG	GCTCGTCTCTGTGGTCTTCT
Per1	TGACATAACCAGGTGCCGTCCA	CAGTCCACACACGCCATCACA
Per2	CCAGGCGGTGTTGAAGGAGGA	CCTCTATCCTGGGGCTGTCA
Ppara	GGCTGCTATAATTTGCTGTGGAG	TGTGTACGAGCTGCCCATGC
Ppard	CCGCAAGCCCTTCAGTGACATCAT	GCAGATGGAATTCTAGAGCCCGCA
Pparg	TGCGGAAGCCCTTTGGTGACT	ATGTCCTCGATGGGCTTCACGTTTC
Rev-erba	CCGCACAACCTACAGTCTGCA	GTTGTTACAGGTCCCGCATGC
Scd1	AGCCTGTTTCGTTAGCACCTTC	ACTCCCGTCTCCAGTTCTCTT
Slc27a2	TGAGGGTCCGAATTGGGATGGC	TTCCATCAGGGTCACTTTGGC
Slc27a5	GCTCCCTGCCATGCCACACC	CACACACAGCCTGGTACACAT
Srebp1c	CGGCGCGGAAGCTGTCGGGGT	TGTCTTGGTTGTGATGAGTGGA

Aacs, acetoacetyl-coenzyme A synthetase; Acaca, acetyl-coenzyme A carboxylase alpha; Acadm, acyl-coenzyme A dehydrogenase, medium chain; Agpat2, 1-acylglycerol-3-phosphate *O*-acyltransferase 2; Agpat6, 1-acylglycerol-3-phosphate *O*-acyltransferase 6; Cpt1a, carnitine palmitoyltransferase 1a; Dbp, D site albumin promoter binding protein; Dgat2, diacylglycerol *O*-acyltransferase 2; Elovl6, ELOVL family member 6, elongation of long chain fatty acids; Gpat1, glycerol-3-phosphate acyltransferase, mitochondrial; Hmgcr, 3-hydroxy-3-methylglutaryl-coenzyme A reductase; Ldlr, low density lipoprotein receptor; Scd1, stearoyl-coenzyme A desaturase 1; Slc27a2, solute carrier family 27 (fatty acid transporter) member 2; Slc27a5, solute carrier family 27 (fatty acid transporter) member 5; Srebp1c, sterol-regulatory element binding protein 1c.

Isolation and circadian synchronization of primary hepatocytes

Primary hepatocytes were isolated as described (44) with some modifications. Livers were isolated and injected with collagenase digestion buffer: Krebs-Ringer-HEPES buffer (121 mM NaCl, 4.9 mM KCl, 1.2 mM MgSO₄, 0.33 mM CaCl₂, 12 mM HEPES, pH 7.4) containing 0.1% collagenase IV, 1% BSA, and 6 mM glucose. The injected livers were incubated at 37°C for 30 min, filtered through a 500 μ m metal mesh to remove undigested tissue, and centrifuged at 50 *g* for 5 min at 4°C. The cells were washed once with cold William's E medium and cultured in Willman's E medium containing 10% FBS, 0.1 μ M insulin, and 0.1 μ M dexamethasone (Dex) for 4 days. The cells were detached with a treatment of 0.25% trypsin-EDTA and seeded in 12-well plates (5×10^5 cells/well) in growth medium (DMEM containing 10% FBS). After a 2 h incubation with growth medium containing 100 nM Dex the following day, the medium was replaced with growth medium and samples were collected every 4 h.

Transfection of hepatocytes

Primary hepatocytes (15×10^5 cells/well) were cultured in 6-well plates and transfected with siRNAs (60 μ M) using Lipofectamine (Invitrogen) the following day. Transfected cells were treated with 0.25% trypsin-EDTA to detach the cells and plated to 12-well plates (5×10^5 cells/well) the following day. The cells were synchronized with 100 nM Dex after 16 h of growth. For hepatocyte TG measurement, cells (5×10^5 cells/well) were seeded in 12-well plates and transfected with siRNAs (30 μ M) or

plasmids (0.5 μ g). Cells were lysed 48 h posttransfection in buffer containing 1% Triton-X100, and TG concentrations were measured as described for hepatic TG. For gene expression analysis, cells were seeded in 12-well plates and transfected with siRNAs (30 μ M) or plasmids (0.5 μ g). Transfected cells were synchronized with 100 nM Dex after 40 h of growth, and RNA samples were collected.

mRNA decay assays

Primary hepatocytes were treated with actinomycin D (5 μ g/ml), and RNA was isolated at different time points. Levels of mRNAs were analyzed by quantitative PCR (qPCR). Wild-type and *Ksrp*^{-/-} mouse embryonic fibroblasts (MEFs) were transfected with globin mRNA reporters in 6-well plates. Transfected cells were pooled and replated to 12-well plates the following day. Cells were treated with actinomycin D (5 μ g/ml) 36 h after transfection, and RNA was isolated at different time points. Levels of reporter mRNAs were analyzed by qPCR using specific primers for human β -globin gene and normalized by β -actin mRNA levels.

Ribonucleoprotein immunoprecipitation assays

Ribonucleoprotein immunoprecipitation (RIP) assays were performed as described (45, 46). Briefly, cell lysates were immunoprecipitated with protein A/protein G beads coupled with anti-KSRP serum at 4°C overnight. Pellets were washed eight times, and RNA was isolated from the immunocomplex using TRIzol, reverse transcribed, and amplified by RT-PCR.

RNA binding assays

³²P-labeled RNAs were in vitro transcribed from PCR-amplified fragments containing a T7 RNA polymerase promoter. RNA binding and UV-cross-linking assays and immunoprecipitation of RNA-protein complexes were previously described (42).

Immunoprecipitation, immunoblotting, and antibodies

Cells or tissues were lysed in RIPA buffer (0.5% NP-40, 0.5% sodium deoxycholate, 0.1% SDS, 150 mM NaCl, 50 mM Tris-Cl, pH 7.5). For detection of PER2, PER2 was immunoprecipitated with rabbit polyclonal antibodies (Alpha Diagnostic International), and the immunoprecipitates were separated on a 7% SDS-PAGE and probed with guinea pig anti-PER2 antibodies (KeraFast). For immunoblotting, proteins were separated on a 7–10% SDS-PAGE, transferred to a polyvinylidene difluoride membrane, and probed with following antibodies: anti-CLOCK (Cell Signaling), anti-BMAL1 (Bethyl Laboratories Inc.), anti-KSRP (47), anti-FLAG (Sigma), anti- α -tubulin (Sigma), and anti-Myc (Roche Diagnostics).

Plasmids

Constructs that expressed Flag-tagged KSRP and Myc-tagged PER2 were described previously (48, 49). A construct, pcDNA3-hGB, expressing human β -globin mRNA, was previously described (50). Fragments of *Per2* 3' UTR were amplified by PCR and subcloned into *NotI* and *XbaI* sites of pcDNA3-hGB. Potential AU-rich regions were mutated by PCR-mediated site-directed mutagenesis, and mutations were confirmed by DNA sequencing.

siRNAs

SiGENOME SMART pool siRNA against *Per2* was purchased from Thermo Scientific. A control siRNA was purchased from Qiagen.

Statistical analysis

All data are presented as the mean \pm SEM. Statistical significance (*P* value) was calculated by unpaired two-tailed Student's *t*-test or one-way ANOVA.

RESULTS

KSRP ablation causes a reduction in hepatic and serum TG contents

We have previously shown that *Ksrp*^{-/-} mice exhibit reduced adiposity due to increased fat utilization in white adipose tissue (51, 52). As the liver also plays a key role in lipid metabolism, we examined TG levels in the liver and serum of *Ksrp*^{-/-} mice under fed and fasting conditions. On a chow diet (NCD), fed and fasting hepatic TG levels were significantly reduced in *Ksrp*^{-/-} mice compared with wild-type mice (Fig. 1A). While no difference in fasting serum TG concentrations was detected between the groups, fed serum TG levels were also reduced in *Ksrp*^{-/-} mice (Fig. 1B). When fed a HFD, *Ksrp*^{-/-} mice showed a 30–50% reduction in hepatic TG levels under both fed and fasting conditions (Fig. 1A). HFD-fed *Ksrp*^{-/-} mice also displayed lower fed serum TG levels (Fig. 1B). Unlike TG levels, no difference in hepatic cholesterol levels was observed between wild-type and *Ksrp*^{-/-} mice (Fig. 1C). However, *Ksrp*^{-/-} mice showed lower fed serum cholesterol levels on an NCD and an HFD and lower fasting serum cholesterol levels on an HFD, although the difference was smaller than that in TG levels (Fig. 1D). These data indicate that KSRP ablation reduces hepatic and serum TG levels and protects from diet-induced hepatic steatosis.

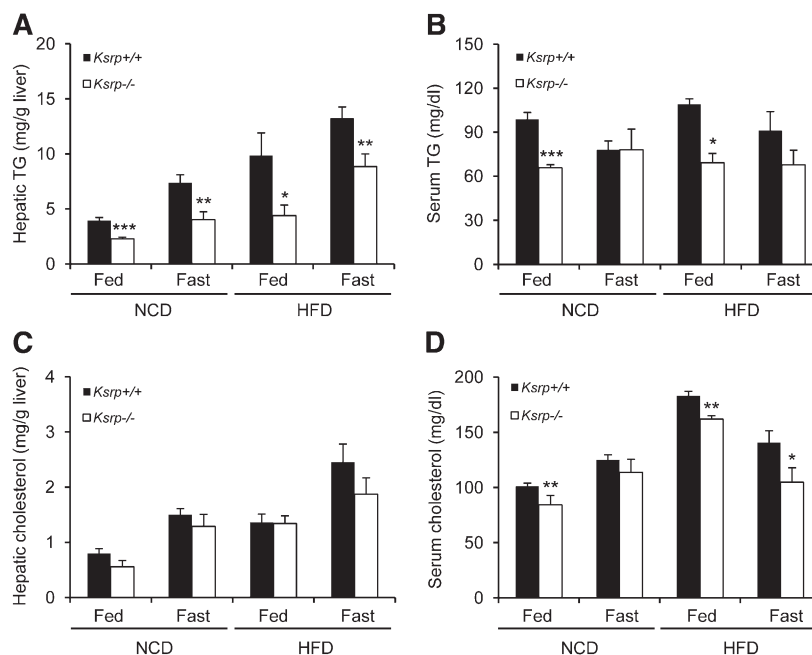


Fig. 1. Reduced hepatic and serum TG levels in *Ksrp*^{-/-} mice. A: Hepatic TG levels of NCD- and HFD-fed wild-type and *Ksrp*^{-/-} mice under fed and fasting conditions (n = 6–8 per group). B: Serum TG levels of NCD- and HFD-fed wild-type and *Ksrp*^{-/-} mice under fed and fasting conditions (n = 6–8 per group). C: Hepatic cholesterol levels of NCD- and HFD-fed wild-type and *Ksrp*^{-/-} mice under fed and fasting conditions (n = 6–8 per group). D: Serum total cholesterol levels of NCD- and HFD-fed wild-type and *Ksrp*^{-/-} mice under fed and fasting conditions (n = 6–8 per group). Data are mean \pm SEM. * *P* < 0.05, ** *P* < 0.01, and *** *P* < 0.005.

***Per2* expression is elevated, and oscillations of circadian clock genes are altered in *Ksrp*^{-/-} liver**

As disturbance in circadian regulation of lipid metabolism in the liver alters TG content, we tested whether KSRP ablation results in altered circadian clocks and examined diurnal expression of core clock genes in livers of wild-type and *Ksrp*^{-/-} mice. While the abundance of most canonical core clock genes was not affected, *Per2* mRNA levels were significantly elevated in *Ksrp*^{-/-} livers compared with wild-type in the dark period (Fig. 2A). We also observed a phase shift (delayed by ~4 h) in the oscillations of several core clock genes including *Per1*, *Clock*, *Rev-erba*, *Bmal1* (while the delay of *Bmal1* was moderate), and *Dbp* (a direct target of CLOCK/BMAL1) in *Ksrp*^{-/-} livers (Fig. 2A). By contrast, no shift was observed for *Cry1* and *Cry2* (Fig. 2A). PER2 protein levels in *Ksrp*^{-/-} livers were also increased in the light and dark periods (Fig. 2B) while the levels of CLOCK and BMAL1 were not altered (Fig. 2C). In addition, KSRP showed a diurnal expression with higher expression levels between ZT8 and ZT16 (Fig. 2C). Unlike that in the livers, *Per2* mRNA levels were not altered in *Ksrp*^{-/-} epididymal white adipose tissue (eWAT) (Fig. 2D). No significant difference in core clock gene expression was observed in *Ksrp*^{-/-} eWAT compared with wild-type, although the levels of *Clock* mRNA were moderately elevated in the light period and there was a shift in the peak of *Cry1* mRNA (Fig. 2D). Thus, these results indicate that absence of KSRP enhances *Per2*

expression and causes a delay in the oscillating phases of several core clock genes in the liver.

***Ksrp*^{-/-} mice display an altered clock function**

To test whether KSRP is also required for central clock function, we measured wheel-running behavior of wild-type and *Ksrp*^{-/-} mice. *Ksrp*^{-/-} mice exhibited typical entrainment to the light cycles compared with wild-type mice in LD (Fig. 3A). In DD, *Ksrp*^{-/-} mice showed a moderately lengthened free-running period (wild-type = 23.7 h vs. *Ksrp*^{-/-} = 23.9 h; Fig. 3A, B). We examined the expression of clock genes in the SCN at the day time (ZT6) and the night time (ZT18) and observed a moderate increase in expression of *Per2* and *Cry1* at ZT18 and *Clock* at ZT6 in *Ksrp*^{-/-} mice while expression of most clock genes was not affected (Fig. 3C). Because the circadian clock plays an important role in determining patterns of food intake and feeding behavior exhibits a pronounced circadian rhythmicity, we monitored diurnal rhythms of food intake. There was no significant difference in feeding behavior between wild-type and *Ksrp*^{-/-} mice (Fig. 3D). These results suggest that KSRP moderately regulates the central clock and is required for maintaining a normal circadian period.

Circadian oscillations and expression of some lipid metabolism genes are altered in *Ksrp*^{-/-} liver

To understand the molecular basis leading to reduced hepatic TG levels, we examined diurnal expression of lipid

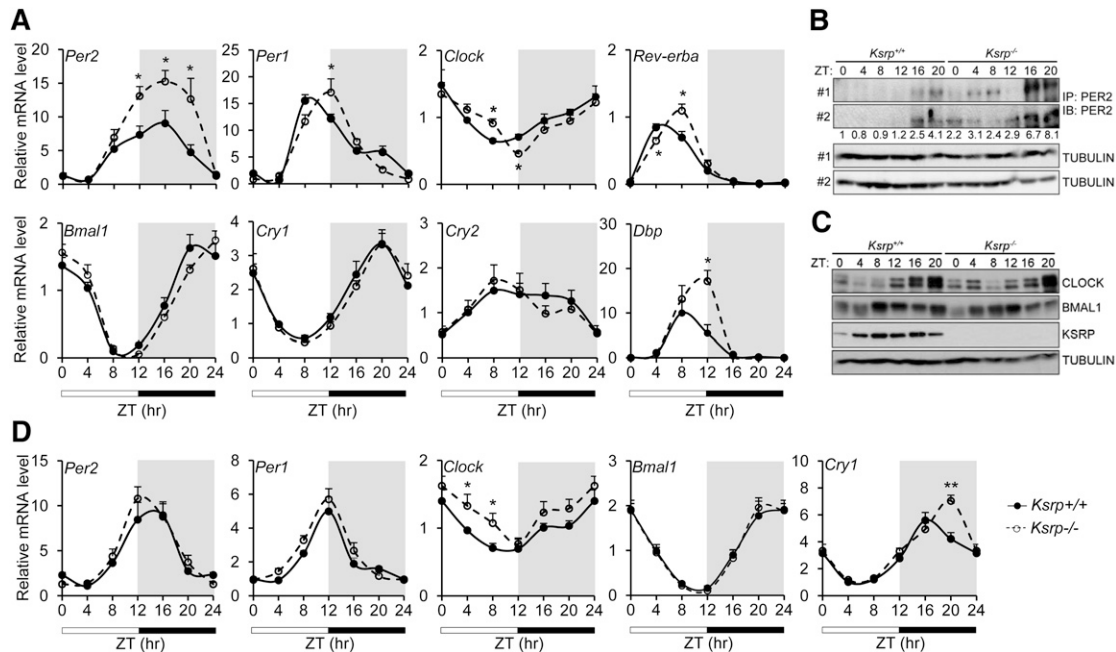


Fig. 2. KSRP ablation upregulates *Per2* and causes a phase shift in oscillations of some circadian clock genes in *Ksrp*^{-/-} livers, but not eWAT. **A:** Circadian oscillations of *Per2*, *Per1*, *Clock*, *Rev-erba*, *Bmal1*, *Cry1*, *Cry2*, and *Dbp* in wild-type and *Ksrp*^{-/-} livers. RNA was isolated from livers of wild-type (n = 6) and *Ksrp*^{-/-} (n = 6) mice at different ZTs (ZT0: lights on; ZT12: lights off), and gene expression was analyzed by qPCR. The ZT0 values were plotted twice as ZT0 and ZT24. Data are mean ± SEM. **P* < 0.05 between groups at each time point. **B:** Liver extracts were immunoprecipitated (IP) with anti-PER2 antibodies, and the immunoprecipitates were analyzed by immunoblotting (IB) using anti-PER2 antibodies. Pooled liver extracts of two mice were analyzed for each time point. Two independent IP/IB analyses using different mice are shown. α-Tubulin levels in the inputs of IP were used as a loading control. Quantification of PER2 levels is indicated. Data are the mean of two IP/IB experiments. **C:** Liver extracts of two mice for each time point were analyzed by immunoblotting using anti-CLOCK, anti-BMAL1, anti-KSRP, and anti-α-tubulin. **D:** Circadian oscillations of *Per2*, *Per1*, *Clock*, *Bmal1*, and *Cry1* in wild-type and *Ksrp*^{-/-} eWAT (n = 4). Data are mean ± SEM. **P* < 0.05 and ***P* < 0.01 between groups at each time point.

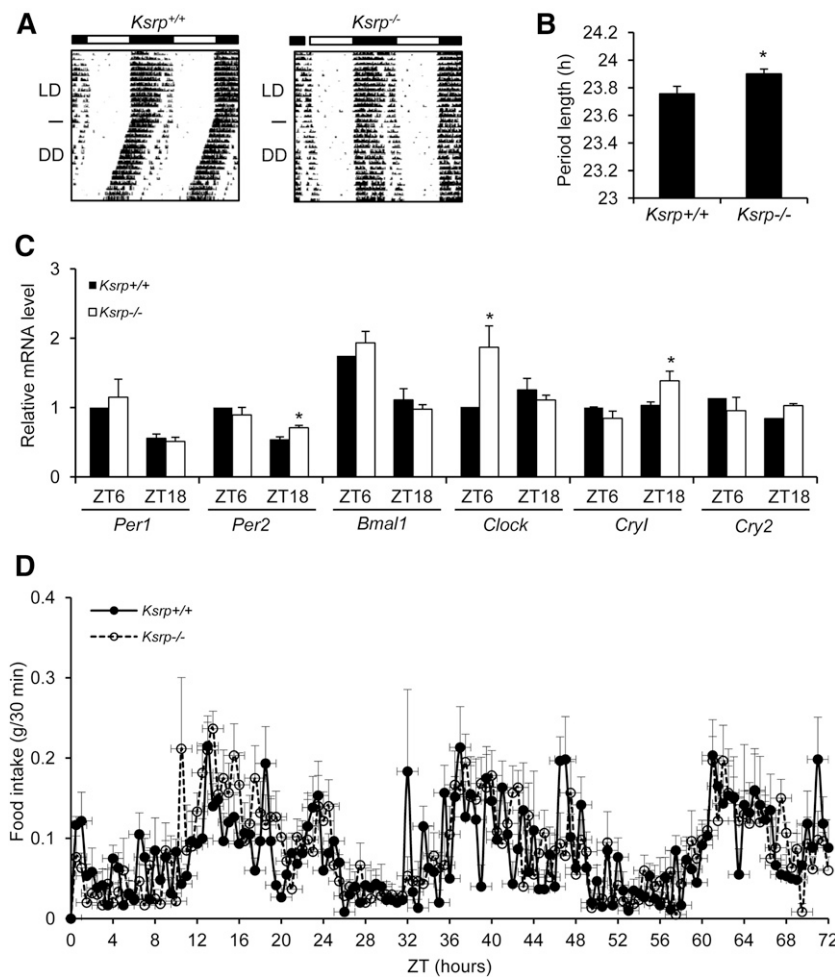


Fig. 3. Disrupted clock function in *Ksrp*^{-/-} mice. **A:** Locomotor activity of wild-type and *Ksrp*^{-/-} mice under a normal 12:12 LD cycle and under DD. Data were plotted in duplicates. **B:** Free-running periods of wild-type and *Ksrp*^{-/-} mice were calculated from **A** (n = 10 for each group). **C:** Expression of *Per1*, *Per2*, *Bmal1*, *Clock*, *Cry1*, and *Cry2* in wild-type and *Ksrp*^{-/-} SCN at ZT6 and ZT18 (n = 3 for each genotype and each time point). Data are mean ± SEM. * *P* < 0.05. **D:** Food intake of wild-type and *Ksrp*^{-/-} mice under a normal 12:12 LD cycle was monitored over three consecutive 24 h cycles. Results are mean ± SEM (n = 6 per genotype).

metabolism genes involved in de novo fatty acid synthesis (*Acaca*, *Fasn*, *Scd1*, and *Elovl6*), TG synthesis (*Gpat1*, *Agpat2*, *Agpat6*, and *Dgat2*), fatty acid uptake (*Cd36*, *Scl27a2*, *Scl27a5*, and *Ldlr*), fatty acid oxidation (*Cpt1a* and *Acadm*), and cholesterol synthesis (*Aacs* and *Hmgcr*) in wild-type and *Ksrp*^{-/-} livers. Expression of genes involved in fatty acid synthesis, including *Acaca*, *Fasn*, *Scd1*, and *Elovl6*, and TG synthesis, including *Agpat2* and *Agpat6*, either was decreased or showed a phase shift in the livers of *Ksrp*^{-/-} mice (Fig. 4A, B), suggesting that either lipogenesis is attenuated or its timing is shifted. We also observed a reduction in expression of *Cd36* and a significant phase shift in cycling of *Scl27a2* and *Ldlr* (Fig. 4C), suggesting that lipid uptake may be altered in *Ksrp*^{-/-} livers. Expression of *Acadm* was increased and cycling of *Aacs* and *Hmgcr* was delayed (Fig. 4D), suggesting that fatty acid oxidation may be increased and cholesterol synthesis is also affected in *Ksrp*^{-/-} livers. We next examined expression profiles of master regulators of lipid metabolism including *Ppara*, *Ppard*, *Pparg*, and *Srebp1c*. While no alteration in expression of *Ppara* and *Ppard* was observed, expression of *Pparg* and *Srebp1c* was

significantly attenuated with a phase shift in the oscillation of *Pparg* in *Ksrp*^{-/-} livers (Fig. 4E). These data indicate that KSRP deficiency results in either phase shift in oscillations or reduced expression of several lipid metabolism genes in the liver. The reduction is particularly concentrated on the genes encoding enzymes involved in de novo lipogenesis likely due to a reduction in expression of their upstream regulators such as *Pparg* and *Srebp1c*.

Per2 expression is elevated and oscillations of some clock genes are phase shifted in primary *Ksrp*^{-/-} hepatocytes

To determine whether the altered circadian rhythms in *Ksrp*^{-/-} liver are cell autonomous, we prepared primary hepatocytes and synchronized the cells with Dex, which induces oscillations of core clock genes in cell lines (53). *Per2* mRNA levels were elevated at 24 h and thereafter after Dex treatment in *Ksrp*^{-/-} hepatocytes (Fig. 5A). Oscillating phases of *Rev-erba*, *Bmal1*, and *Per1* were delayed by 4 h in *Ksrp*^{-/-} hepatocytes, although the mRNA abundance was not altered (Fig. 5A). In contrast, no difference in oscillations of *Cry1*, *Cry2*, *Clock*, and *Dbp* was observed between the

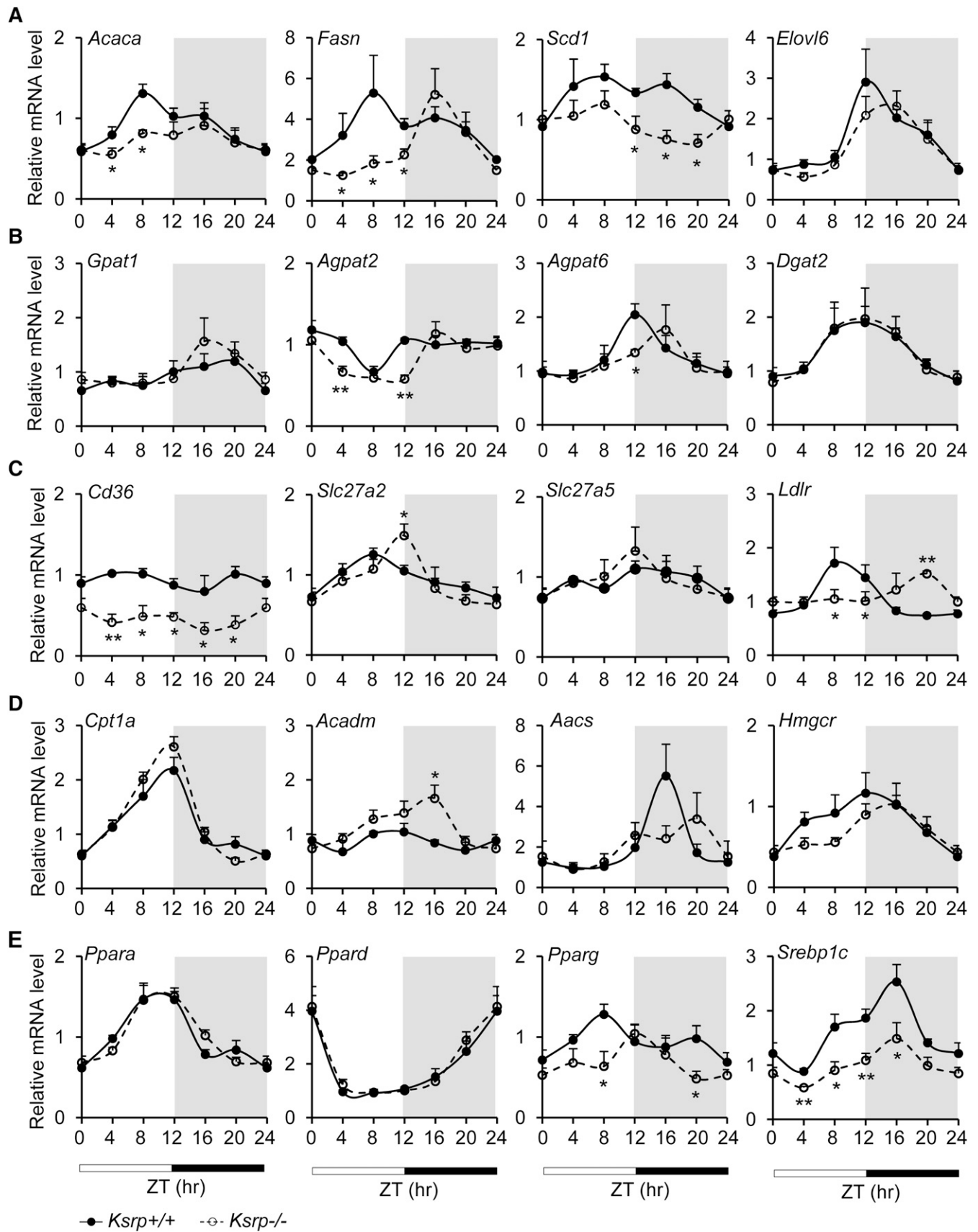


Fig. 4. Oscillations and expression of some lipid metabolism genes are altered in *Ksrp*^{-/-} livers. A: Circadian expression of genes involved in de novo fatty acid synthesis, *Acaca*, *Fasn*, *Scd1*, and *Elovl6*, in wild-type and *Ksrp*^{-/-} livers. B: Circadian expression of genes involved in TG synthesis, *Gpat1*, *Agpat2*, *Agpat6*, and *Dgat2*, in wild-type and *Ksrp*^{-/-} livers. C: Circadian expression of genes involved in lipid uptake, *Cd36*, *Slc27a2*, *Slc27a5*, and *Ldlr*, in wild-type and *Ksrp*^{-/-} livers. D: Circadian expression of genes involved in fatty acid oxidation,

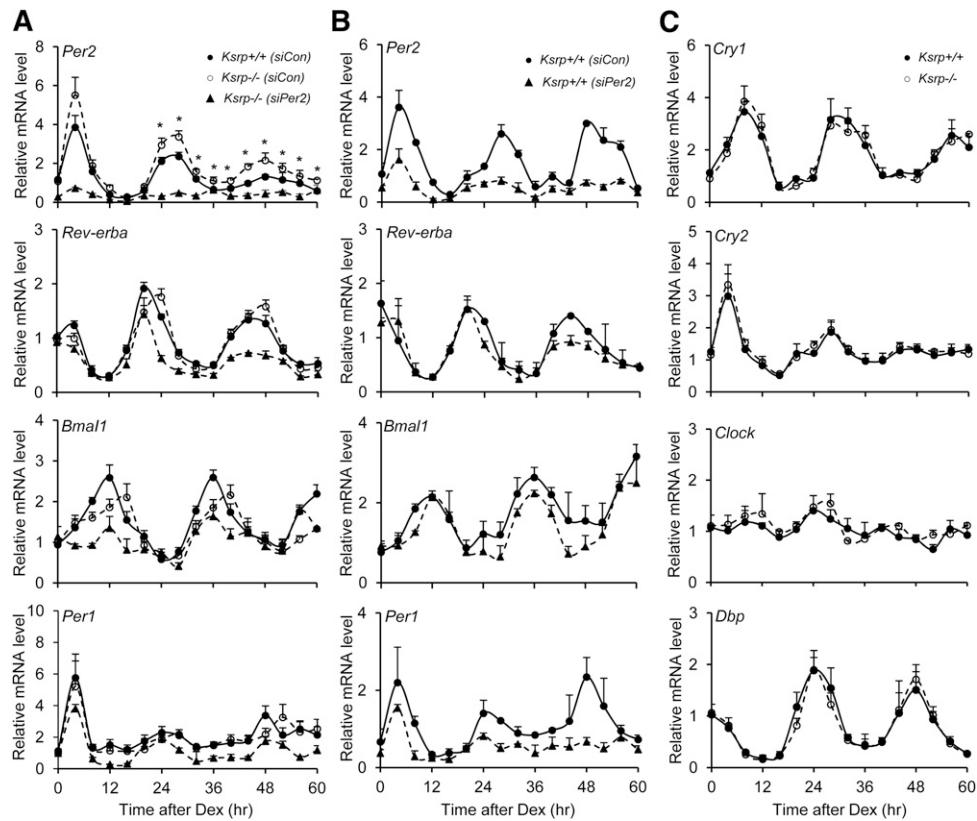


Fig. 5. Upregulation of *Per2* and delayed phases in oscillations of clock genes in *Ksrp*^{-/-} hepatocytes, and downregulation of *Per2* restores the phase shift in oscillations of circadian clock genes in *Ksrp*^{-/-} hepatocytes. A: Oscillations of *Per2*, *Rev-erba*, *Bmal1*, and *Per1* in wild-type hepatocytes transfected with a control siRNA (siCon) and in *Ksrp*^{-/-} hepatocytes transfected with siCon or *Per2* siRNAs (siPer2). * *P* < 0.05 between *Ksrp*^{+/-} (siCon) and *Ksrp*^{-/-} (siCon) at each time point. B: Oscillations of *Per2*, *Rev-erba*, *Bmal1*, and *Per1* in wild-type hepatocytes transfected with siCon or siPer2. C: Oscillations of *Cry1*, *Cry2*, *Clock*, and *Dbp* in wild-type and *Ksrp*^{-/-} hepatocytes. All data are mean ± SEM from three independent preparations of hepatocytes (n = 6).

groups (Fig. 5C). These data strongly implicate that upregulation of *Per2* and phase shift in several circadian clock genes in *Ksrp*^{-/-} livers are cell autonomous and unlikely due to changes in the behavior of *Ksrp*^{-/-} mice.

Downregulation of *Per2* in *Ksrp*^{-/-} hepatocytes reverses delayed circadian clock

We next examined whether increased *Per2* expression leads to altered oscillations of clock genes. Knockdown of *Per2* by siRNAs (siPer2) in *Ksrp*^{-/-} hepatocytes restored the delayed phases of *Rev-erba*, *Bmal1*, and *Per1* similar to that of wild-type hepatocytes, although downregulation of *Per2* also decreased their levels (Fig. 5A). Knockdown of *Per2* in wild-type hepatocytes also attenuated the expression of *Rev-erba*, *Bmal1*, and *Per1* but did not alter their circadian profiles (Fig. 5B), indicating that the rhythmicity in core clock gene expression is retained with reduced *Per2* levels. These data suggest that the phase delay in oscillations of *Rev-erba*, *Bmal1*, and *Per1* in *Ksrp*^{-/-} hepatocytes is indeed due to increased *Per2* expression.

Per2 mRNA decay rate is decreased in *Ksrp*^{-/-} hepatocytes

To determine the underlying mechanism leading to elevated *Per2* expression in the absence of KSRP, we examined decay of *Per2* mRNA in hepatocytes treated with Dex for 32 h (*Per2* mRNA levels are the highest at this time point). As shown in Fig. 6A, *Per2* mRNA stability was increased in *Ksrp*^{-/-} hepatocytes compared with wild type. In contrast, the stability of *Per1* and *Rev-erba* mRNAs, while exhibiting mRNA instability, was not changed between the two groups (Fig. 6B, C). To determine whether KSRP promotes *Per2* mRNA decay by binding to the mRNA, we performed RIP assays. *Per2* mRNA was enriched in the anti-KSRP immunoprecipitate of wild-type liver extracts compared with either a control immunoprecipitate of wild-type extracts or an anti-KSRP immunoprecipitate using *Ksrp*^{-/-} extracts (Fig. 6D). In contrast, no enrichment of *Rev-erba* and β -actin mRNAs was observed in the anti-KSRP immunoprecipitate of wild-type extracts (Fig. 6D). We also examined the interaction of KSRP with *Per2* mRNA

Cpt1a and *Acadm*, and cholesterol synthesis, *Aacs* and *Hmgcr*, in wild-type and *Ksrp*^{-/-} livers. E: Circadian oscillations of *Ppara*, *Ppard*, *Pparg*, and *Srebp1c* in wild-type and *Ksrp*^{-/-} livers. All data are mean ± SEM (n = 6–8 for each genotype). * *P* < 0.05 and ** *P* < 0.01 between groups at each time point.

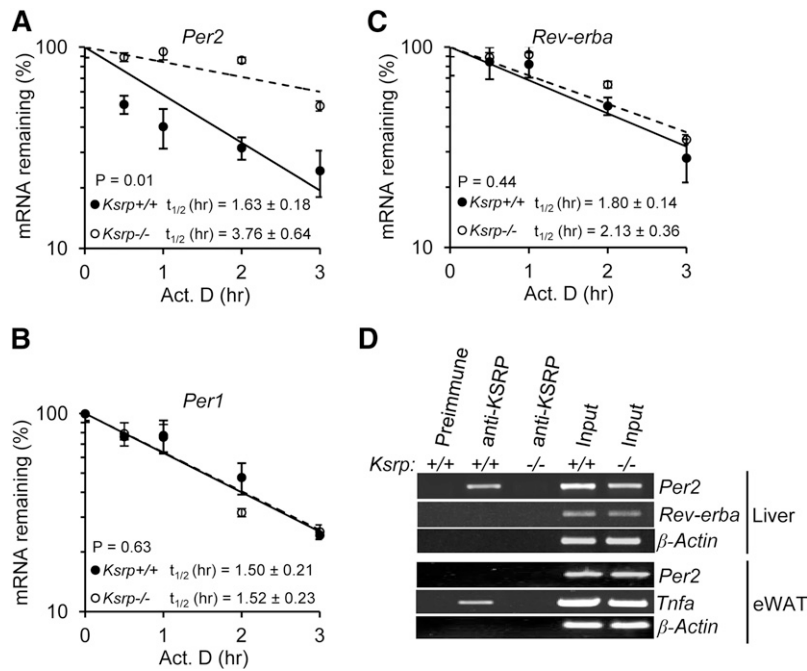


Fig. 6. KSRP controls *Per2* mRNA stability through a direct RNA-protein interaction. A, B, and C: Half-lives of *Per2* mRNA (A), *Per1* mRNA (B), and *Rev-erba* mRNA (C) in wild-type and *Ksrp*^{-/-} hepatocytes. Hepatocytes were treated with actinomycin D (Act. D), and RNA was isolated at different time points after the treatment. mRNA levels of *Per2*, *Per1*, and *Rev-erba* were analyzed by qPCR. The mRNA decay rates were plotted, and the half-lives (*t*_{1/2}) were indicated. Each time point represents mean ± SEM (*n* = 3). D: Association of *Per2* mRNA with KSRP. Liver extracts were prepared from wild-type and *Ksrp*^{-/-} mice and subjected to immunoprecipitation with preimmune serum or anti-KSRP serum. RNA was isolated from the precipitation. The presence of *Per2*, *Rev-erba*, and *β-Actin* mRNAs was analyzed by RT-PCR and agarose gel electrophoresis. eWAT extracts were also prepared from wild-type and *Ksrp*^{-/-} mice and subjected to immunoprecipitation with preimmune serum or anti-KSRP serum. The presence of *Per2*, *Tnfa*, and *β-Actin* mRNAs in the immunoprecipitates was analyzed. Input: RT-PCR reaction of RNA (10% of amounts used for IP) from each genotype.

in eWAT extracts. Consistent with the results in Fig. 2D in which similar *Per2* mRNA levels were detected between wild-type and *Ksrp*^{-/-} eWATs, no KSRP-*Per2* mRNA complex was detected, while *Tnfa* mRNA, a positive control for KSRP-bound RNAs, was detected in the anti-KSRP immunoprecipitate of wild-type extracts (Fig. 6D). These results suggest that KSRP targets *Per2* mRNA for decay by an RNA-protein interaction and upregulation of *Per2* is due to decreased mRNA decay in the absence of KSRP.

KSRP promotes decay of *Per2* mRNA through interaction with the ARE in the 3' UTR

KSRP promotes mRNA decay through direct binding to the AREs in the 3' UTRs of its target mRNAs. To examine the role of KSRP in promoting *Per2* mRNA decay, we subcloned two fragments of *Per2* 3' UTR into the 3' UTR of human β -globin reporter. hGB-*Per2*₁₂₄₁ contains a proximal fragment composed of nucleotides 3,948 to 5,189 (accession #NM_011066) and hGB-*Per2*₆₆₉ contains a distal fragment consisting of nucleotides 5,169 to 5,837 (Fig. 7A). These reporter mRNAs were expressed and their decay rates were monitored in wild-type and *Ksrp*^{-/-} MEFs. The mRNA with the distal fragment (hGB-*Per2*₆₆₉) displayed a half-life (*t*_{1/2}) of 3.6 h (Fig. 7B) in wild-type MEFs. In contrast, the mRNA with the proximal region (hGB-*Per2*₁₂₄₁) did not show any significant decay compared with a control globin mRNA with GAPDH 3' UTR (Fig. 7B). Importantly, decay of hGB-*Per2*₆₆₉ mRNA was impaired in *Ksrp*^{-/-} MEFs (Fig. 7B). These results suggest that the distal region of *Per2* 3' UTR directs mRNA decay and KSRP is responsible for the decay.

There are three potential AREs, AU1, AU2, and AU3, present in the distal region (Fig. 7A). We mutated each ARE and examined mRNA decay. While mutations of AU1 and AU3 did not alter the decay rate compared with hGB-*Per2*₆₆₉ mRNA in wild-type MEFs, mutation of AU2 impaired mRNA decay (Fig. 7C). In addition, all three mutated

mRNAs showed similar mRNA stability in *Ksrp*^{-/-} MEFs (Fig. 7C) suggesting that AU2 mediates KSRP-dependent decay of *Per2* mRNA. RNA binding and UV cross-linking assays showed that an RNA-KSRP complex, which was immunoprecipitated with anti-KSRP, was formed with AU2 RNA using wild-type extracts. By contrast, no RNA-KSRP complex was formed using *Ksrp*^{-/-} extracts (Fig. 7E). While KSRP bound AU1 RNA weakly, it bound AU2 RNA with a high affinity (Fig. 7F). No RNA-KSRP complexes were detected with AU3 RNA and AU2 RNA containing mutations in the ARE (Fig. 7F). Altogether, these data suggest that KSRP promotes *Per2* mRNA decay through the interaction with the AU2 region.

Lipogenic genes are downregulated in *Ksrp*^{-/-} hepatocytes, and downregulation of *Per2* in *Ksrp*^{-/-} hepatocytes restores lipogenic gene expression and TG levels

We examined expression of lipogenic genes in wild-type and *Ksrp*^{-/-} hepatocytes and were unable to detect circadian oscillations in expression of most of these genes in Dex-treated hepatocytes (data not shown). Thus, we examined their expression levels before and 28 h and 32 h after Dex treatment (when *Per2* expression is rising and declining, respectively). Expression of *Acaca* and *Scd1* was decreased in *Ksrp*^{-/-} hepatocytes compared with wild-type both 28 h and 32 h after Dex treatment. Importantly, downregulation of *Per2* restored their expression in *Ksrp*^{-/-} hepatocytes (Fig. 8A). Similar results were detected for *Fasn* 28 h after Dex treatment (Fig. 8A). Downregulation of *Per2* in wild-type hepatocytes did not affect expression of lipogenic genes (Fig. 8A), suggesting that a reduction in *Per2* expression was unable to cause disturbance in lipogenic gene expression. We also observed a reduction in expression of *Srebp1c* both 28 h and 32 h after Dex treatment and reduced expression of *Pparg* before and 28 h after Dex treatment in *Ksrp*^{-/-} hepatocytes (Fig. 8B). Downregulation of *Per2* increased their mRNA levels

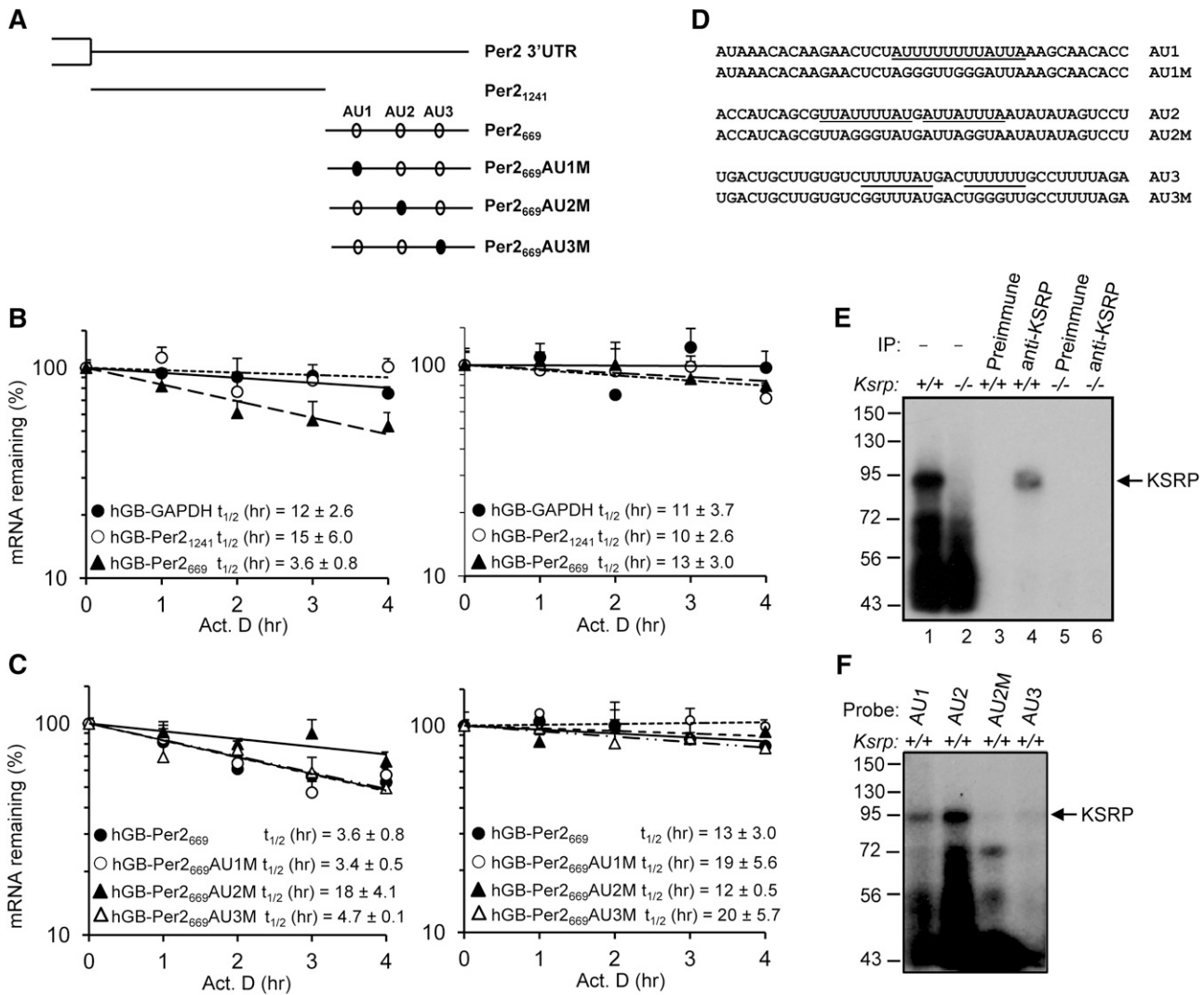


Fig. 7. KSRP controls *Per2* mRNA stability through an interaction with the ARE in the 3' UTR. **A:** Schematic diagram showing the 3' UTR of *Per2*, which is divided into two subregions and subcloned into human β -globin mRNA reporter (hGB-Per2₁₂₄₁ and hGB-Per2₆₆₉). Open ovals indicate AU-rich motifs and mutations of AU motifs are denoted as closed ovals. **B:** Wild-type and *Ksrp*^{-/-} MEFs were transfected with plasmids expressing globin reporters containing the 3' UTR of GAPDH, the proximal region, or distal region of *Per2* 3' UTR and treated with actinomycin D (Act. D). RNA was isolated at different time points after the treatment. mRNA levels of globin reporters were analyzed by qPCR. The mRNA decay rates were plotted and the $t_{1/2}$ were indicated. Each time point represents mean \pm SEM ($n = 6$). **C:** Half-lives of globin mRNAs containing mutations in each AU-rich region in wild-type and *Ksrp*^{-/-} MEFs. **D:** Sequences of AU1, AU2, AU3, and their mutations. AU-rich motifs are underlined. **E:** KSRP interacts with AU2 of *Per2* mRNA. Wild-type or *Ksrp*^{-/-} extracts were incubated with ³²P-labeled AU2 RNA and subjected to UV cross-linking. The RNA-protein complexes were either directly analyzed by SDS-PAGE (lanes 1 and 2) or subjected to immunoprecipitation with preimmune serum (lanes 3 and 5) or anti-KSRP serum (lanes 4 and 6), and then the immunoprecipitates were analyzed by SDS-PAGE and autoradiography. **F:** Interactions of KSRP with AU1, AU2, AU2M, and AU3 RNAs analyzed by UV cross-linking using wild-type MEF extracts.

in *Ksrp*^{-/-} hepatocytes and *Srebp1c* mRNA levels in wild-type cells (Fig. 8B), suggesting that PER2 negatively regulates *Srebp1c* and *Pparg* expression. We next examined intracellular TG levels in wild-type and *Ksrp*^{-/-} hepatocytes. TG levels were decreased in *Ksrp*^{-/-} hepatocytes (Fig. 8C). Downregulation of *Per2* restored TG levels in *Ksrp*^{-/-} hepatocytes to that of wild type, but did not affect TG levels in wild-type hepatocytes (Fig. 8C). We analyzed knockdown efficiency of *Per2* in wild-type and *Ksrp*^{-/-} hepatocytes; the mRNA and protein levels were reduced by ~ 50 – 80% and by $\sim 50\%$, respectively, in wild-type and *Ksrp*^{-/-} cells treated with siPer2 (Fig. 8D, E). Altogether, these results strongly suggest that KSRP deficiency attenuates

the expression of *Srebp1c* and *Pparg*, master regulators of lipogenesis, which is a result of increased *Per2* expression. The reduction in both *Srebp1c* and *Pparg* results in attenuated expression of lipogenic enzymes including *Acaca*, *Fasn*, and *Scd1* and reduced intracellular TG levels.

Overexpression of KSRP decreases *Per2* and increases lipogenic gene expression, and conversely, overexpression of *Per2* downregulates lipogenic gene expression

To further explore the roles of KSRP and PER2 in lipogenic gene expression, we first overexpressed KSRP in wild-type hepatocytes and examined expression of clock and lipogenic genes. Ectopic expression of KSRP decreased

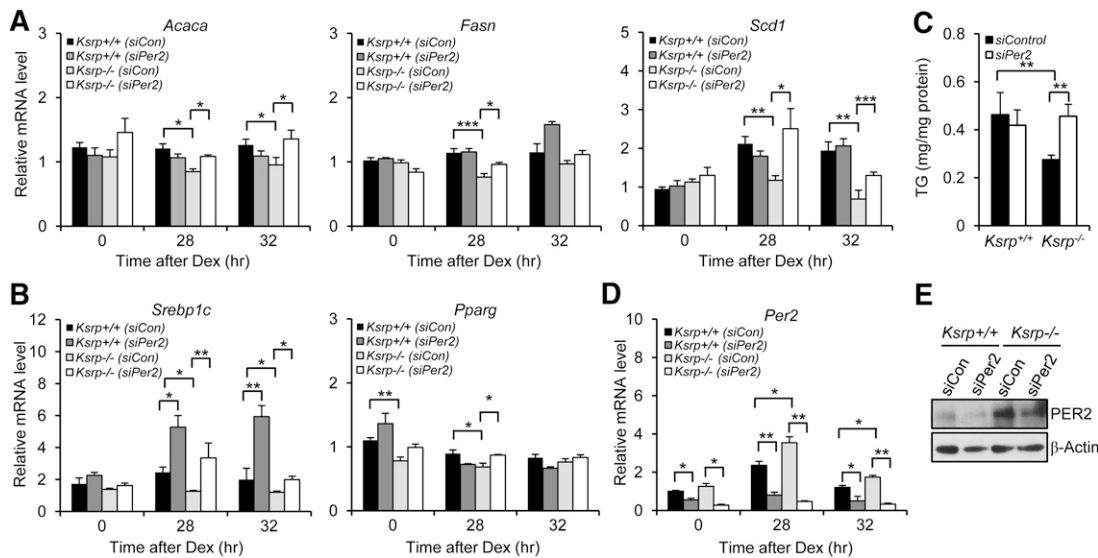


Fig. 8. Downregulation of *Per2* increases lipogenic gene expression and TG levels in *Ksrp*^{-/-} hepatocytes. A: Expression of lipogenic genes, *Acaca*, *Fasn*, and *Scd1*, in wild-type and *Ksrp*^{-/-} hepatocytes transfected with siCon or siPer2 before and 28 h and 32 h after Dex treatment. B: Expression of *Srebp1c* and *Pparg* in wild-type and *Ksrp*^{-/-} hepatocytes transfected with siCon or siPer2 before and 28 h and 32 h after Dex treatment. C: Intracellular TG levels in wild-type and *Ksrp*^{-/-} hepatocytes transfected with siCon or siPer2. All data are mean \pm SEM (n = 4–6). * $P < 0.05$, ** $P < 0.01$, and *** $P < 0.005$. D: Expression of *Per2* in wild-type and *Ksrp*^{-/-} hepatocytes transfected with siCon or siPer2 before and 28 h and 32 h after Dex treatment. E: Wild-type and *Ksrp*^{-/-} hepatocytes were transfected with siCon or siPer2. PER2 expression was analyzed by immunoblotting.

expression of *Per2*, but not *Per1*, *Clock*, *Bmal1*, and *Cry1* (Fig. 9B), and increased expression of *Srebp1c*, *Pparg*, *Acacs*, *Fasn*, and *Scd1* (Fig. 9C). Consistent with the induction of lipogenic genes, overexpression of KSRP moderately increased

intracellular TG levels (Fig. 9F). We next overexpressed PER2 in wild-type hepatocytes to a level similar to that of *Ksrp*^{-/-} hepatocytes (Fig. 9D). Ectopic expression of PER2 in wild-type hepatocytes decreased expression of *Srebp1c*,

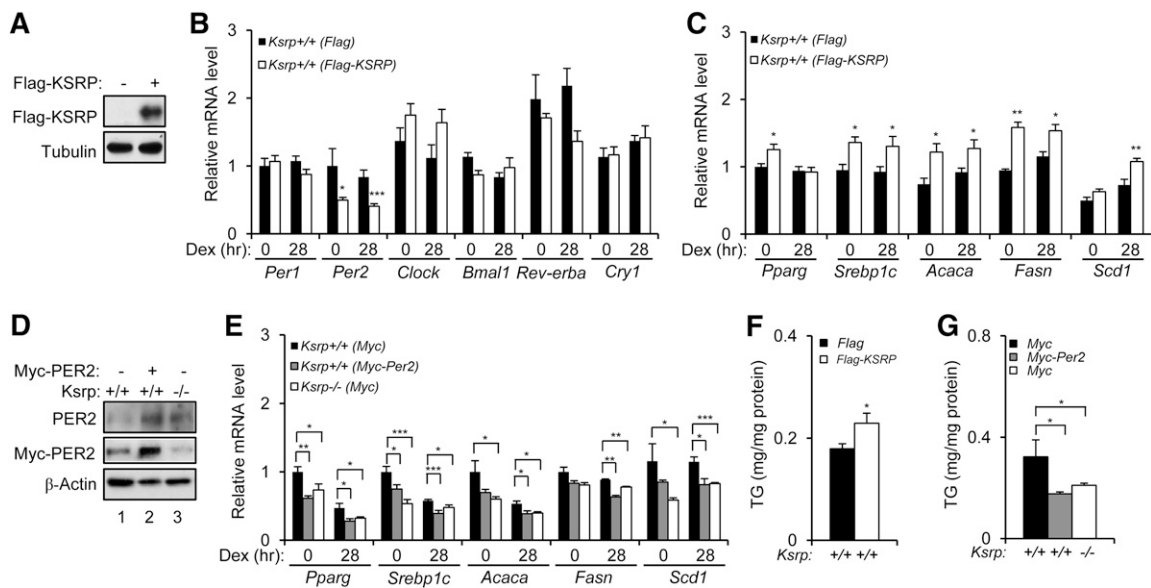


Fig. 9. Overexpression of KSRP decreases *Per2* and increases lipogenic gene expression and overexpression of *Per2* downregulates lipogenic genes. A: Wild-type hepatocytes were transfected with a control plasmid or a construct expressing Flag-tagged KSRP. Expression of Flag-KSRP was analyzed by immunoblotting. The blot was reprobbed with anti- α -tubulin antibody. B: Expression of *Per1*, *Per2*, *Clock*, *Bama1*, *Rev-erba*, and *Cry1* in wild-type hepatocytes expressing Flag-KSRP. C: Expression of *Srebp1c*, *Pparg*, *Acaca*, *Fasn*, and *Scd1* in wild-type hepatocytes expressing Flag-KSRP. D: Wild-type hepatocytes were transfected with a control plasmid or a construct expressing Myc-tagged PER2, and *Ksrp*^{-/-} hepatocytes were transfected with a control plasmid. Total levels of PER2 were analyzed by anti-PER2 immunoblotting. Myc-PER2 levels were also analyzed by anti-Myc immunoprecipitation followed by anti-PER2 immunoblotting. The weak bands detected in the anti-Myc immunoprecipitates in lanes 1 and 3 are likely due to a protein comigrated with Myc-PER2 and cross-reacted with anti-PER2 antibody. The blot was reprobbed with anti- β -actin antibody. E: Expression of *Srebp1c*, *Pparg*, *Acaca*, *Fasn*, and *Scd1* in wild-type hepatocytes with or without expression of Myc-PER2 and *Ksrp*^{-/-} hepatocytes. F and G: Intracellular TG levels in wild-type hepatocytes expressing Flag-KSRP (F) and in wild-type hepatocytes expressing Myc-PER2 and *Ksrp*^{-/-} hepatocytes (G). All data are mean \pm SEM (n = 4–6). * $P < 0.05$, ** $P < 0.01$, and *** $P < 0.005$.

Pparg, *Acacs*, *Fasn*, and *Scd1* (Fig. 9E) and TG levels (Fig. 9F) to similar levels to that of *Ksrp*^{-/-} hepatocytes. These results suggest that KSRP negatively regulates *Per2* expression and PER2 downregulates the expression of lipogenic genes.

DISCUSSION

This study shows that KSRP ablation causes a reduction in hepatic TG content. At the molecular level, we found that *Per2* gene is upregulated and diurnal expression of several core clock genes is phase shifted in the livers of *Ksrp*^{-/-} mice. Similar to the disturbance in liver clock, daily cycling of lipid metabolism genes is disrupted with either a phase shift or reduced expression of enzymes and master regulators, such as *Pparg* and *Srebp1c*, involved in de novo lipogenesis. Using primary hepatocytes of *Ksrp*^{-/-} mice, we demonstrated that downregulation of *Per2* reverses the phase shift in oscillations of clock genes and restores the downregulation of lipogenic genes. These results suggest that increased expression of *Per2* in *Ksrp*^{-/-} hepatocytes results in downregulation of *Pparg* and *Srebp1c*, thereby reducing lipogenesis and TG content, and that KSRP plays a critical role in lipid metabolism through regulation of *Per2* expression in the liver.

SREBP1c is a transcription factor that increases lipogenesis by promoting expression of lipogenic genes such as *Acaca*, *Fasn*, and *Scd1*. The critical role of SREBP1c in hepatic lipogenesis is supported by gain- and loss-of-function studies showing that overexpression of an active form develops steatosis as a result of elevation of lipogenesis, and conversely deficiency of hepatic SREBP1c fails to induce lipogenic gene expression (54). PPAR γ activates genes involved in lipid storage and metabolism. Whereas it is expressed mostly in adipose tissue, liver-specific knockout of *Pparg* reduces expression of *Acaca*, *Fasn*, and *Scd1* and hepatic steatosis (55, 56). These results implicate that PPAR γ -regulated lipogenesis also plays a vital role in regulation of TG content in the liver. Furthermore, genetic studies have also demonstrated that mice with liver ablation of *Acaca* and *Scd1* have reduced liver TG levels (57, 58). These findings demonstrate a role of de novo lipogenesis in contributing to hepatic steatosis and support our hypothesis that the reduced TG content in the livers of *Ksrp*^{-/-} mice is at least partly attributed to attenuated hepatic lipogenesis. However, we cannot exclude that reduced or altered fatty acid uptake also contributes a reduction in TG content as expression of *Cd36*, *Slc27a2*, and *Ldlr* is either decreased or phase shifted in *Ksrp*^{-/-} livers (Fig. 4C).

We showed that downregulation of *Per2* restored expression of *Srebp1c* and *Pparg* in *Ksrp*^{-/-} primary hepatocytes. Conversely, ectopic expression of *Per2* in wild-type hepatocytes reduced expression of *Srebp1c* and *Pparg*. These data implicate that PER2 negatively regulates *Srebp1c* and *Pparg*. It is currently unclear how PER2 achieves the repression. In a direct role, PER2 may negatively regulate transcription of *Srebp1c* and *Pparg* independent of its ability to control circadian gene expression in the liver. Previous studies demonstrated that PER2 is able


to control lipid metabolism by inhibiting PPAR γ function in adipocytes through direct protein-protein interactions (49). However, it is unknown whether PER2 transcriptionally regulates *Pparg* expression. It was shown that disruption of Clock function affects daily rhythmicity in the expression of *Srebp1c* in the liver (59) and that the CLOCK/BMAL1 complex binds to the promoter sequence of *Srebp1c* (28). Thus, it is possible that PER2 represses transcription of *Srebp1c* through a negative regulation of transcriptional activity of CLOCK/BMAL1 (28).

In an indirect role, PER2 may regulate the circadian clock, which in turn regulates diurnal expression of lipid metabolism genes. The upregulation of *Per2* in *Ksrp*^{-/-} liver may cause dysregulation or misalignment of the liver clock with feeding behavior and/or nutritional state resulting in altered accumulation of hepatic TG. Previous reports support this hypothesis. While ablation of clock genes, such as *Clock*, *Bmal1*, *Rev-erba*, *Rev-erba/Rev-erbb*, *Per1/Per2*, and *Cry1/Cry2* results in altered accumulation of hepatic TG, there is no consistency regarding to an increase or a decrease in TG levels (19, 28, 29, 31, 32, 60). Furthermore, some lipid related genes still exhibited circadian oscillations in *Per1/2*-null livers (31) indicating that the circadian expression of these genes is under both clock-dependent and clock-independent fashions and responds to feeding. Thus, the altered hepatic TG levels in a variety of mouse models with clock gene ablation likely result from a misalignment of circadian expression of lipid metabolism genes with nutritional state responding to feeding behavior. However, one cannot exclude the possibility that each clock component has a direct role in controlling lipid metabolism independent of the ability to regulate the circadian clock. While we cannot rule out that the reduction of TG contents in *Ksrp*^{-/-} livers is due to an alteration in nutritional state, but not altered rhythmic expression of clock and lipid metabolism genes, we found that diurnal food intake is not altered in *Ksrp*^{-/-} mice. The exact mechanism that leads to reduced hepatic TG levels through increased *Per2* expression awaits further studies.

We showed that downregulation of *Per2* in *Ksrp*^{-/-} hepatocytes to a level similar to wild-type level restored the phase delay in cycling of clock genes and TG levels while 50% reduction of *Per2* in wild-type cells did not alter clock gene expression and TG levels (Fig. 5 and Fig. 8). Although we did not examine oscillation of remaining PER2 protein in wild-type and *Ksrp*^{-/-} cells after the knockdown, *Per2* mRNA levels remain oscillating (Fig. 5). These findings suggest that the remaining PER2 in wild-type cells is able to maintain normal oscillations of clock genes and that the effects on cycling of clock genes and TG accumulation in *Ksrp*^{-/-} cells is indeed due to increased PER2. We found that both *Per2* knockdown and KSRP overexpression increased *Srebp1c* in wild-type cells (Fig. 8B and Fig. 9C). However, only the mRNA levels of *Acaca*, *Fasn*, and *Scd1* and TG were increased in KSRP-overexpressed cells. It is currently unclear what causes the discrepancy as these lipid genes are targets of SREBP1c. One likely explanation is that SREBP1c is not limited or whose activity is restricted in wild-type cells. Thus, the increase in SREBP1c upon *Per2* knockdown is not able

to further activate its target genes, whereas other genes that modulate SREBP1c activity are also affected by KSRP overexpression, thereby enhancing its transcriptional activity. It is also possible that the increase in lipogenesis through KSRP overexpression is independent of *Srebp1c* upregulation and *Per2* downregulation.

We observed an elevation of *Per2* mRNA levels due to increased mRNA stability in the absence of KSRP and demonstrated that AU2 is responsible for KSRP-dependent mRNA decay (Fig. 7). The effect of KSRP ablation on *Per2* mRNA levels was only observed in the liver but not in eWAT, suggesting a tissue-specific role of KSRP in controlling *Per2* mRNA stability. Consistent with this, KSRP-*Per2* mRNA complex is not detected in eWAT. It is possible that the decay-promoting activity of KSRP toward *Per2* mRNA in eWAT can be redundantly conferred by other decay-promoting ARE binding proteins that also promote decay of ARE-containing mRNAs (61, 62). These additional ARE binding proteins likely compete with KSRP for interaction with the AREs of *Per2* mRNA in eWAT.

While *Ksrp*^{-/-} mice have reduced hepatic TG content, it will be of interest to see whether the attenuated expression of lipogenic genes and de novo lipogenesis is attributed to the liver-specific function of KSRP and whether the increase in *Per2* expression indeed contributes the observed effects. Further studies using mice with liver-specific ablation of KSRP, and mice with both KSRP ablation and liver-specific knockout of *Per2* should provide insights into these questions. In summary, this work demonstrates a novel function of KSRP in hepatic lipid metabolism and suggests that reduction in hepatic de novo lipogenesis through modulation of KSRP activity could be a potential therapeutic target for hepatosteatosis. However, targeting KSRP might also affect several other pathways as it is also found in apoB editing catalytic component I complex (63, 64) and pri-miRNA processing complex (35). KSRP inhibition may alter apoB mRNA editing causing an alteration in blood lipoprotein profiles. As miRNAs are involved in a variety of cellular pathways, more dramatic outcomes would be anticipated upon KSRP suppression. Thus, the clinical utility of KSRP suppression to control hepatic lipogenesis may be dampened, and this approach needs to be carefully evaluated. Several potential approaches could be envisioned: 1) targeting KSRP specifically in the liver as other pathways regulated in different tissues are not affected; 2) suppressing the ability of KSRP to interact with ARE-containing mRNAs, but not pri-miRNA binding ability; and 3) suppressing the ability of KSRP to recruit mRNA decay machineries. 

The authors thank Dr. P. Sassone-Corsi for a Myc-*Per2* construct.

REFERENCES

- Abdelmalek, M. F., and A. M. Diehl. 2007. Nonalcoholic fatty liver disease as a complication of insulin resistance. *Med. Clin. North Am.* **91**: 1125–1149.
- Lewis, J. R., and S. R. Mohanty. 2010. Nonalcoholic fatty liver disease: a review and update. *Dig. Dis. Sci.* **55**: 560–578.
- Postic, C., and J. Girard. 2008. Contribution of de novo fatty acid synthesis to hepatic steatosis and insulin resistance: lessons from genetically engineered mice. *J. Clin. Invest.* **118**: 829–838.
- Ferré, P., and F. Foufelle. 2010. Hepatic steatosis: a role for de novo lipogenesis and the transcription factor SREBP-1c. *Diabetes Obes. Metab.* **12** (Suppl. 2): 83–92.
- Kawano, Y., and D. E. Cohen. 2013. Mechanisms of hepatic triglyceride accumulation in non-alcoholic fatty liver disease. *J. Gastroenterol.* **48**: 434–441.
- Lewis, G. F., A. Carpentier, K. Adeli, and A. Giacca. 2002. Disordered fat storage and mobilization in the pathogenesis of insulin resistance and type 2 diabetes. *Endocr. Rev.* **23**: 201–229.
- Shearman, L. P., S. Sriram, D. R. Weaver, E. S. Maywood, I. Chaves, B. Zheng, K. Kume, C. C. Lee, G. T. van der Horst, M. H. Hastings, et al. 2000. Interacting molecular loops in the mammalian circadian clock. *Science*. **288**: 1013–1019.
- Reppert, S. M., and D. R. Weaver. 2002. Coordination of circadian timing in mammals. *Nature*. **418**: 935–941.
- Ko, C. H., and J. S. Takahashi. 2006. Molecular components of the mammalian circadian clock. *Hum. Mol. Genet.* **15**: R271–R277.
- King, D. P., Y. Zhao, A. M. Sangoram, L. D. Wilsbacher, M. Tanaka, M. P. Antoch, T. D. Steeves, M. H. Vitaterna, J. M. Kornhauser, P. L. Lowrey, et al. 1997. Positional cloning of the mouse circadian clock gene. *Cell*. **89**: 641–653.
- Gekakis, N., D. Staknis, H. B. Nguyen, F. C. Davis, L. D. Wilsbacher, D. P. King, J. S. Takahashi, and C. J. Weitz. 1998. Role of the CLOCK protein in the mammalian circadian mechanism. *Science*. **280**: 1564–1569.
- Kume, K., M. J. Zylka, S. Sriram, L. P. Shearman, D. R. Weaver, X. Jin, E. S. Maywood, M. H. Hastings, and S. M. Reppert. 1999. mCRY1 and mCRY2 are essential components of the negative limb of the circadian clock feedback loop. *Cell*. **98**: 193–205.
- Bunger, M. K., L. D. Wilsbacher, S. M. Moran, C. Clendenin, L. A. Radcliffe, J. B. Hogenesch, M. C. Simon, J. S. Takahashi, and C. A. Bradfield. 2000. Mop3 is an essential component of the master circadian pacemaker in mammals. *Cell*. **103**: 1009–1017.
- Zheng, B., U. Albrecht, K. Kaasik, M. Sage, W. Lu, S. Vaishnav, Q. Li, Z. S. Sun, G. Eichele, A. Bradley, et al. 2001. Nonredundant roles of the mPer1 and mPer2 genes in the mammalian circadian clock. *Cell*. **105**: 683–694.
- Lee, E. C., D. Yu, J. Martinez de Velasco, L. Tessarollo, D. A. Swing, D. L. Court, N. A. Jenkins, and N. G. Copeland. 2001. A highly efficient Escherichia coli-based chromosome engineering system adapted for recombinogenic targeting and subcloning of BAC DNA. *Genomics*. **73**: 56–65.
- Okamura, H., S. Miyake, Y. Sumi, S. Yamaguchi, A. Yasui, M. Muijtjens, J. H. Hoeijmakers, and G. T. van der Horst. 1999. Photic induction of mPer1 and mPer2 in cry-deficient mice lacking a biological clock. *Science*. **286**: 2531–2534.
- Sato, T. K., R. G. Yamada, H. Ukai, J. E. Baggs, L. J. Miraglia, T. J. Kobayashi, D. K. Welsh, S. A. Kay, H. R. Ueda, and J. B. Hogenesch. 2006. Feedback repression is required for mammalian circadian clock function. *Nat. Genet.* **38**: 312–319.
- Preitner, N., F. Damiola, L. Lopez-Molina, J. Zakany, D. Duboule, U. Albrecht, and U. Schibler. 2002. The orphan nuclear receptor REV-ERB α controls circadian transcription within the positive limb of the mammalian circadian oscillator. *Cell*. **110**: 251–260.
- Turek, F. W., C. Joshu, A. Kohsaka, E. Lin, G. Ivanova, E. McDearmon, A. Laposky, S. Losee-Olson, A. Easton, D. R. Jensen, et al. 2005. Obesity and metabolic syndrome in circadian Clock mutant mice. *Science*. **308**: 1043–1045.
- Marcheva, B., K. M. Ramsey, E. D. Buhr, Y. Kobayashi, H. Su, C. H. Ko, G. Ivanova, C. Omura, S. Mo, M. H. Vitaterna, et al. 2010. Disruption of the clock components CLOCK and BMAL1 leads to hypoinsulinaemia and diabetes. *Nature*. **466**: 627–631.
- Green, C. B., J. S. Takahashi, and J. Bass. 2008. The meter of metabolism. *Cell*. **134**: 728–742.
- Asher, G., and U. Schibler. 2011. Crosstalk between components of circadian and metabolic cycles in mammals. *Cell Metab.* **13**: 125–137.
- Bass, J. 2012. Circadian topology of metabolism. *Nature*. **491**: 348–356.
- Panda, S., M. P. Antoch, B. H. Miller, A. I. Su, A. B. Schook, M. Straume, P. G. Schultz, S. A. Kay, J. S. Takahashi, and J. B. Hogenesch. 2002. Coordinated transcription of key pathways in the mouse by the circadian clock. *Cell*. **109**: 307–320.
- Zvonic, S., A. A. Pitsyn, S. A. Conrad, L. K. Scott, Z. E. Floyd, G. Kilroy, X. Wu, B. C. Goh, R. L. Mynatt, and J. M. Gimble. 2006.

- Characterization of peripheral circadian clocks in adipose tissues. *Diabetes*. **55**: 962–970.
26. Storch, K. F., O. Lipan, I. Leykin, N. Viswanathan, F. C. Davis, W. H. Wong, and C. J. Weitz. 2002. Extensive and divergent circadian gene expression in liver and heart. *Nature*. **417**: 78–83.
 27. McCarthy, J. J., J. L. Andrews, E. L. McDearmon, K. S. Campbell, B. K. Barber, B. H. Miller, J. R. Walker, J. B. Hogenesch, J. S. Takahashi, and K. A. Esser. 2007. Identification of the circadian transcriptome in adult mouse skeletal muscle. *Physiol. Genomics*. **31**: 86–95.
 28. Shimba, S., T. Ogawa, S. Hitosugi, Y. Ichihashi, Y. Nakadaira, M. Kobayashi, M. Tezuka, Y. Kosuge, K. Ishige, Y. Ito, et al. 2011. Deficient of a clock gene, brain and muscle Arnt-like protein-1 (BMAL1), induces dyslipidemia and ectopic fat formation. *PLoS ONE*. **6**: e25231.
 29. Bugge, A., D. Feng, L. J. Everett, E. R. Briggs, S. E. Mullican, F. Wang, J. Jager, and M. A. Lazar. 2012. Rev-erbalpha and Rev-erdbeta coordinately protect the circadian clock and normal metabolic function. *Genes Dev*. **26**: 657–667.
 30. Feng, D., T. Liu, Z. Sun, A. Bugge, S. E. Mullican, T. Alenghat, X. S. Liu, and M. A. Lazar. 2011. A circadian rhythm orchestrated by histone deacetylase 3 controls hepatic lipid metabolism. *Science*. **331**: 1315–1319.
 31. Adamovich, Y., L. Rouso-Noori, Z. Zwighaft, A. Neufeld-Cohen, M. Golik, J. Kraut-Cohen, M. Wang, X. Han, and G. Asher. 2014. Circadian clocks and feeding time regulate the oscillations and levels of hepatic triglycerides. *Cell Metab*. **19**: 319–330.
 32. Cretenet, G., M. Le Clech, and F. Gachon. 2010. Circadian clock-coordinated 12 Hr period rhythmic activation of the IRE1alpha pathway controls lipid metabolism in mouse liver. *Cell Metab*. **11**: 47–57.
 33. Min, H., C. W. Turck, J. M. Nikolic, and D. L. Black. 1997. A new regulatory protein, KSRP, mediates exon inclusion through an intronic splicing enhancer. *Genes Dev*. **11**: 1023–1036.
 34. Gherzi, R., K. Y. Lee, P. Briata, D. Wegmuller, C. Moroni, M. Karin, and C. Y. Chen. 2004. A KH domain RNA binding protein, KSRP, promotes ARE-directed mRNA turnover by recruiting the degradation machinery. *Mol. Cell*. **14**: 571–583.
 35. Trabucchi, M., P. Briata, M. Garcia-Mayoral, A. D. Haase, W. Filipowicz, A. Ramos, R. Gherzi, and M. G. Rosenfeld. 2009. The RNA-binding protein KSRP promotes the biogenesis of a subset of microRNAs. *Nature*. **459**: 1010–1014.
 36. Dhamija, S., N. Kuehne, R. Winzen, A. Doerrie, O. Dittrich-Breiholz, B. K. Thakur, M. Kracht, and H. Holtmann. 2011. Interleukin-1 activates synthesis of interleukin-6 by interfering with a KH-type splicing regulatory protein (KSRP)-dependent translational silencing mechanism. *J. Biol. Chem*. **286**: 33279–33288.
 37. Chen, C. Y., R. Gherzi, S. E. Ong, E. L. Chan, R. Rajmakers, G. J. Pruijn, G. Stoecklin, C. Moroni, M. Mann, and M. Karin. 2001. AU binding proteins recruit the exosome to degrade ARE-containing mRNAs. *Cell*. **107**: 451–464.
 38. Winzen, R., B. K. Thakur, O. Dittrich-Breiholz, M. Shah, N. Redich, S. Dhamija, M. Kracht, and H. Holtmann. 2007. Functional analysis of KSRP interaction with the AU-rich element of interleukin-8 and identification of inflammatory mRNA targets. *Mol. Cell. Biol*. **27**: 8388–8400.
 39. Briata, P., S. V. Forcales, M. Ponassi, G. Corte, C. Y. Chen, M. Karin, P. L. Puri, and R. Gherzi. 2005. p38-Dependent phosphorylation of the mRNA decay-promoting factor KSRP controls the stability of select myogenic transcripts. *Mol. Cell*. **20**: 891–903.
 40. Briata, P., C. Ilengo, G. Corte, C. Moroni, M. G. Rosenfeld, C. Y. Chen, and R. Gherzi. 2003. The Wnt/beta-catenin→Pitx2 pathway controls the turnover of Pitx2 and other unstable mRNAs. *Mol. Cell*. **12**: 1201–1211.
 41. Gherzi, R., M. Trabucchi, M. Ponassi, T. Ruggiero, G. Corte, C. Moroni, C. Y. Chen, K. S. Khabar, J. S. Andersen, and P. Briata. 2006. The RNA-binding protein KSRP promotes decay of beta-catenin mRNA and is inactivated by PI3K-AKT signaling. *PLoS Biol*. **5**: e5.
 42. Lin, W. J., X. Zheng, C. C. Lin, J. Tsao, X. Zhu, J. J. Cody, J. M. Coleman, R. Gherzi, M. Luo, T. M. Townes, et al. 2011. Posttranscriptional control of type I interferon genes by KSRP in the innate immune response against viral infection. *Mol. Cell. Biol*. **31**: 3196–3207.
 43. Folch, J., M. Lees, and G. H. Sloane Stanley. 1957. A simple method for the isolation and purification of total lipides from animal tissues. *J. Biol. Chem*. **226**: 497–509.
 44. Li, W. C., K. L. Ralphs, and D. Tosh. 2010. Isolation and culture of adult mouse hepatocytes. *Methods Mol. Biol*. **633**: 185–196.
 45. Briata, P., W. J. Lin, M. Giovarelli, M. Pasero, C. F. Chou, M. Trabucchi, M. G. Rosenfeld, C. Y. Chen, and R. Gherzi. 2012. PI3K/AKT signaling determines a dynamic switch between distinct KSRP functions favoring skeletal myogenesis. *Cell Death Differ*. **19**: 478–487.
 46. Pasero, M., M. Giovarelli, G. Bucci, R. Gherzi, and P. Briata. 2012. Bone morphogenetic protein/SMAD signaling orients cell fate decision by impairing KSRP-dependent microRNA maturation. *Cell Reports*. **2**: 1159–1168.
 47. Hall, M. P., S. Huang, and D. L. Black. 2004. Differentiation-induced colocalization of the KH-type splicing regulatory protein with polypyrimidine tract binding protein and the c-src pre-mRNA. *Mol. Biol. Cell*. **15**: 774–786.
 48. Lin, W. J., A. Duffy, and C. Y. Chen. 2007. Localization of AU-rich element-containing mRNA in cytoplasmic granules containing exosome subunits. *J. Biol. Chem*. **282**: 19958–19968.
 49. Grimaldi, B., M. M. Bellet, S. Katada, G. Astarita, J. Hirayama, R. H. Amin, J. G. Granneman, D. Piomelli, T. Leff, and P. Sassone-Corsi. 2010. PER2 controls lipid metabolism by direct regulation of PPARgamma. *Cell Metab*. **12**: 509–520.
 50. Lykke-Andersen, J., M. D. Shu, and J. A. Steitz. 2000. Human Upf proteins target an mRNA for nonsense-mediated decay when bound downstream of a termination codon. *Cell*. **103**: 1121–1131.
 51. Chou, C. F., Y. Y. Lin, H. K. Wang, X. Zhu, M. Giovarelli, P. Briata, R. Gherzi, W. T. Garvey, and C. Y. Chen. 2014. KSRP ablation enhances brown fat gene program in white adipose tissue through reduced miR-150 expression. *Diabetes*. **63**: 2949–2961.
 52. Lin, Y. Y., C. F. Chou, M. Giovarelli, P. Briata, R. Gherzi, and C. Y. Chen. 2014. KSRP and microRNA 145 are negative regulators of lipolysis in white adipose tissue. *Mol. Cell. Biol*. **34**: 2339–2349.
 53. Balsalobre, A., S. A. Brown, L. Marcacci, F. Tronche, C. Kellendonk, H. M. Reichardt, G. Schutz, and U. Schibler. 2000. Resetting of circadian time in peripheral tissues by glucocorticoid signaling. *Science*. **289**: 2344–2347.
 54. Ye, J., and R. A. DeBose-Boyd. 2011. Regulation of cholesterol and fatty acid synthesis. *Cold Spring Harb. Perspect. Biol*. **3**: a004754.
 55. Gavrilova, O., M. Haluzik, K. Matsusue, J. J. Cutson, L. Johnson, K. R. Dietz, C. J. Nicol, C. Vinson, F. J. Gonzalez, and M. L. Reitman. 2003. Liver peroxisome proliferator-activated receptor gamma contributes to hepatic steatosis, triglyceride clearance, and regulation of body fat mass. *J. Biol. Chem*. **278**: 34268–34276.
 56. Matsusue, K., M. Haluzik, G. Lambert, S. H. Yim, O. Gavrilova, J. M. Ward, B. Brewer, Jr., M. L. Reitman, and F. J. Gonzalez. 2003. Liver-specific disruption of PPARgamma in leptin-deficient mice improves fatty liver but aggravates diabetic phenotypes. *J. Clin. Invest*. **111**: 737–747.
 57. Mao, J., F. J. DeMayo, H. Li, L. Abu-Elheiga, Z. Gu, T. E. Shaikenov, P. Kordari, S. S. Chirala, W. C. Heird, and S. J. Wakil. 2006. Liver-specific deletion of acetyl-CoA carboxylase 1 reduces hepatic triglyceride accumulation without affecting glucose homeostasis. *Proc. Natl. Acad. Sci. USA*. **103**: 8552–8557.
 58. Miyazaki, M., M. T. Flowers, H. Sampath, K. Chu, C. Oztzelberger, X. Liu, and J. M. Ntambi. 2007. Hepatic stearoyl-CoA desaturase-1 deficiency protects mice from carbohydrate-induced adiposity and hepatic steatosis. *Cell Metab*. **6**: 484–496.
 59. Matsumoto, E., A. Ishihara, S. Tamai, A. Nemoto, K. Iwase, T. Hiwasa, S. Shibata, and M. Takiguchi. 2010. Time of day and nutrients in feeding govern daily expression rhythms of the gene for sterol regulatory element-binding protein (SREBP)-1 in the mouse liver. *J. Biol. Chem*. **285**: 33028–33036.
 60. Le Martelot, G., T. Claudel, D. Gatfield, O. Schaad, B. Kornmann, G. L. Sasso, A. Moschetta, and U. Schibler. 2009. REV-ERBalpha participates in circadian SREBP signaling and bile acid homeostasis. *PLoS Biol*. **7**: e1000181.
 61. Bevilacqua, A., M. C. Ceriani, S. Capaccioli, and A. Nicolini. 2003. Post-transcriptional regulation of gene expression by degradation of messenger RNAs. *J. Cell. Physiol*. **195**: 356–372.
 62. Barreau, C., L. Paillard, and H. B. Osborne. 2005. AU-rich elements and associated factors: are there unifying principles? *Nucleic Acids Res*. **33**: 7138–7150.
 63. Lellek, H., R. Kirsten, I. Diehl, F. Apostel, F. Buck, and J. Greeve. 2000. Purification and molecular cloning of a novel essential component of the apolipoprotein B mRNA editing enzyme-complex. *J. Biol. Chem*. **275**: 19848–19856.
 64. Lellek, H., S. Welker, I. Diehl, R. Kirsten, and J. Greeve. 2002. Reconstitution of mRNA editing in yeast using a Gal4-apoB-Gal80 fusion transcript as the selectable marker. *J. Biol. Chem*. **277**: 23638–23644.